A 2 × 2 MIMO Throughput Analytical Model for RF Front End Optimization

Penghui Shen, Yihong Qi, Xianbin Wang, Wei Zhang, Wei Yu

***Abstract*—With a given communication protocol, performance optimization of a multiple-input multiple-output (MIMO) wireless system mainly lies on the design of the radio frequency (RF) front end. Currently, the optimization is mainly achieved based on experiences, such as promoting the multiple antenna gains and reducing their correlations. This experience-based method works to a certain extent, but is inefficient since the final performance impact by each sub-system is not quantified. The challenge lies on how to find the most limiting factor that restricts the overall communication throughput. This paper presents an analytical model for throughput calculations of 2 × 2 MIMO wireless system, which is built on a first step of maximum rate calculated under the chosen protocol and channel, followed by a second step of throughput baseline measurement, and continued with the third step of throughput calculations of the overall system according to the actual settings of subsystems. The model can provide a detailed diagnostic report of each RF factor, which will directly point out the imperfections and make the troubleshooting and debugging much more effective. Besides, throughput is analyzed in a mathematical approach that allows the performance more predictable during the design phase.**

Manuscript received Apr. 21, 2020; revised May 29, 2020; accepted May 31, 2020. This work was supported in part by Chinese Ministry of Education—China Mobile Research Foundation under Grant MCM 20150101 and in part by National Natural Science Foundation of China under Grant 61671203. The associate editor coordinating the review of this paper and approving it for publication was L. Bai.

P. H. Shen, Y. H. Qi. College of Electric and Information, Hunan University, Changsha 410082, China (e-mail: penghui.shen@generaltest.com; yihong.qi@generaltest.com).

P. H. Shen, Y. H. Qi, W. Yu. General Test Systems Inc., Shenzhen 518000, China (e-mail: penghui.shen@generaltest.com; yihong.qi@generaltest.com; fred.yu@generaltest.com).

Y. H. Qi. Peng Cheng Laboratory, Shenzhen 518000, China (e-mail: yihong.qi@generaltest.com).

X. B. Wang. Department of Electrical and Computer Engineering, Western University, London, ON N6A 5B9, Canada (e-mail: xianbin.wang@uwo.ca).

W. Zhang. School of Electrical Engineering and Telecommunications, University of New South Wales, Sydney NSW 2052, Australia (e-mail: w.zhang@unsw.edu.au).

***Keywords*—throughput analytical model, MIMO, RF performance optimizations**

I. Introduction

The expeditious evolution of wireless technologies through 1G to 5G has dramatically increased the compelxity of communications systems and networks[1,2]. Performance of an advanced wireless system in 5G era is affected by many factors, ranging from physical layer transmission parameters, wireless channel conditions to the supporting communications protocols[3,4]. Determining the accurate performance of a complex wireless system could be very difficult due to the cascaded effects of so many parameters as well as the real-time interaction among the different layers of the protocol stack. Finding out the factors limiting the overall performance of a wireless system could be even more challenging. However, achieving this would be highly beneficial to improve the overall performance of wireless systems and reduce the product development time.

This particular situation can be explained by Liebig's barrel. One can easily observe the capacity of a barrel with staves of unequal length limited by the shortest stave. This implies that the most effective way to improve the overall performance of a system is to address the most limiting factor (i.e., the shortest stave of the barrel). This motivates us to consider the following question. For a multiple-input multiple-output (MIMO) wireless system, how to find the most limiting factor that restricts the overall communication throughput? Due to its inherent complexity, performance of a MIMO system could be affected by many factors, components and procedures, including but not limited to radio frequency (RF) front-end, noise/interference/signal distortion, modulation and coding in time, frequency and space domains, etc.[5,6]. Among these parameters, extracting the dominating factors on the achievable data rate and modeling their impact could lead to a very valuable diagnosis of a complex communication system. Such efforts could directly guide designers to improve the system performance, which is typically evaluated by system throughput[7,8].

However, decomposition and analysis of a wireless system's throughput has specific difficulties. Studies in

Authorized licensed use limited to: HUNAN UNIVERSITY. Downloaded on March 04,2021 at 08:40:01 UTC from IEEE Xplore. Restrictions apply.

Refs. [9,10] have considered several cases for throughput analysis with ideal RF transceivers, where the impact of coding and modulation on throughput has been discussed. While the related studies have contributed to the performance analysis of communication systems, the actual throughput that a wireless system can achieve is determined not only by transmission schemes, but also by the RF chain and channel for achieving signal propagation from transmitter to receiver. Studies in Refs. [11,12] have discussed the effects on overall performance from antenna correlation to isolation in several representative scenarios, which are useful for separating antenna designing factors. However, the challenge lies on the fact that there is currently no accurate theory to determine wireless system throughput while considering the impacts of RF metrics. Currently, the only reliable way for finding out a wireless system's throughput rate in the Cellular Telecommunications and Internet Association (CTIA) and the 3rd Generation Partnership Project (3GPP) standards is via testing[13,14].

This brings the following challenge to the 5G design engineers. When wireless devices fail to pass the network certification measurements, how to do troubleshooting and decomposition? Generally, subsystems such as MIMO antennas, multiple receivers, desensitization (also called desense) of a system are designed by different departments. The overall performance after system integration may differ substantially from the simply adding up the performance of each component due to the omission of cascaded effects[15-17]. Measured throughput does not indicate the most limiting factor, i.e., where the shortest stave is located. To make the situation even worse, the influence of component improvements on overall performance during the design phase couldn't be assessed without an accurate throughput analytical model. As a result, debugging and troubleshooting for 5G MIMO system becomes an extremely time-consuming, uneffective, and experience-based process.

To solve the issue, an analytical model for 2×2 MIMO throughput is proposed in the paper, which is built on a first step of maximum rate calculated under the chosen protocol and channel, followed by a second step of throughput baseline measurement, and continuing with the third step of throughput calculations of the overall system according to the actual settings of subsystems. The receiver chip throughput performance is first simulated in the model reflecting the limit capability that the entire system can achieve. Then is the performance degradation brought by applied antennas referred to two omnidirectional and uncorrelated MIMO antennas. Finally, the desense-caused degradation is calculated in numbers. It is the first time that the mentioned three values are achievable in the research and development (R&D) stage of a wireless system. Such a diagnostic report makes it possible for engineers to estimate the performance degradation brought to each subsystem during the simulation phase, further significantly reducing the development period.

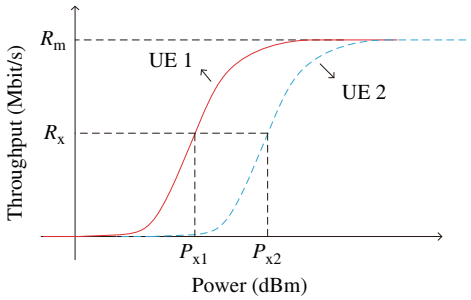

Figure 1 Experiential relationship between a MIMO system's throughput and the downlink power with a selected protocol

The rest of the paper is organized as follows. Section II provides the throughput modeling framework, followed by the throughput model theoretical derivation in section III. In section IV, the accuracy of the model is validated based on practical experiments, and in section V, a typical application of the proposed model is introduced. Finally, the conclusions are presented.

II. Throughput Modeling

An actual data rate is lower than the channel capacity given by Shannon equation because of two reasons. One is protocol, including coding algorithm, modulation process, etc., which always allocates some resources for carrying the supplementary information[18,19]. The maximum throughput, denoting the upper limit that a chosen protocol can support, is marked as the protocol rate in the paper. The protocol rate has been studied for years, and its calculations have been presented in Ref. [10] and Refs. [20,21]. On the other hand, throughput also depends on physical chain performance, including RF metrics and propagation quality. Protocol rate is always greater than or equal to the throughput of a wireless system.

According to the standards[13,14], throughput is defined as the time-averaged number of correctly received transport blocks over a reference mathematical channel. The actual rate is defined in a testing and statistical perspective, and there is no accurate theory to determine a wireless system's actual rate. Experiments show that the relationship between a MIMO system's throughput and the downlink power can be depicted as the solid red line in Fig. 1[13,14,17]. The protocol rate R_m could be achieved while the downlink power is kept at a relative high level (related to the received noise). For different terminals under a same protocol, the throughput function may differ, as shown by the blue dotted line in Fig. 1. The power corresponding to a constant throughput value of R_x $(0 < R_x < R_m)$ is selected as the throughput performance indicator. As shown in Fig. 1, P_{x1} and P_{x2} reflect the performances with the two RF metrics applied respec-

Authorized licensed use limited to: HUNAN UNIVERSITY. Downloaded on March 04,2021 at 08:40:01 UTC from IEEE Xplore. Restrictions apply.

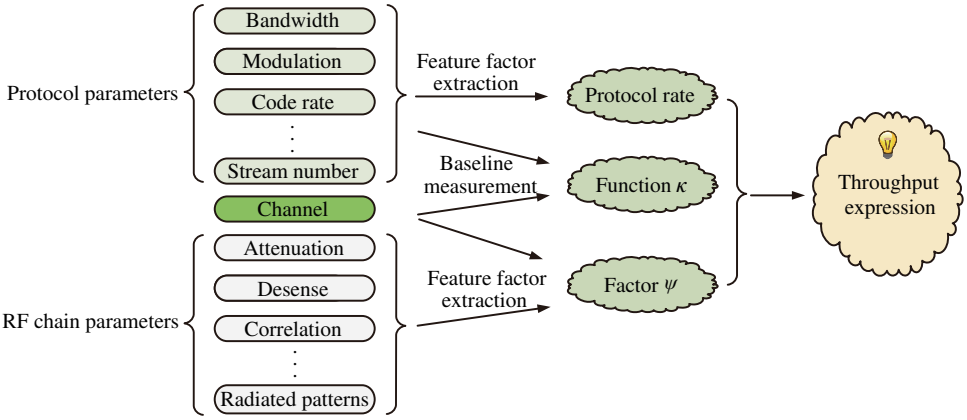

Figure 2 The throughput model is built on three steps: protocol rate achievement, baseline function measurement, and the RF performance related factor calculation

tively. It is clear that the 1st user equipment (UE) has a better performance since a lower power level is required for reaching the same throughput value of R_{x}. Based on experimental measurement results, the paper proposes an analytical model for 2×2 MIMO throughput calculation, which is established on the perspective that with a selected protocol, throughput degradation is only determined by the RF performance of an actual wireless system, as shown in Fig. 1. The model is expressed as

$$T_{\mathrm{pm}} = R_{\mathrm{m}} * \kappa(\mathrm{Snr}), \qquad \mathrm{Snr} = P_{\mathrm{d}} - N_0 + \Psi, \tag{1}$$

where T_{pm} represents the actual throughput; R_{m} is the protocol rate of a 2×2 MIMO system under a chosen protocol (in Mbit/s); κ denotes the throughput function, which is determined by the protocol settings and channel; Snr is the received signal noise ratio (SNR) in format of dB; P_{d} is the downlink power in dBm; N_0 is the received noise at MIMO receivers; Ψ is a factor associated with the RF performance (in dB).

The analytical model is built on two facts. First, with a chosen combination of protocol and channel, the value R_{m} can be calculated by referring to the methods in Refs. [20,21], and the κ function could be achieved via one measurement of a throughput curve. Second, once the RF related factor Ψ is obtained, the throughput value in (1) will be acquired. As shown in Fig. 2, the model is based on a first process of looking up the protocol rate via combining the protocol related information, and followed by a second process of baseline function measurement of κ, considering both the selected protocol and channel, and continued with a third process of Ψ calculation via combining the RF chain factors about desense, antenna patterns, channel, etc. Both R_{m} and κ function are invariable under a chosen protocol and channel, so any change in RF front end can be computed for its corresponding impact of throughput. Therefore, the rest of this paper will mainly focus on the analysis of how RF performance impacts final throughput performance.

III. Modeling of RF Performance Impact on Throughput

For a mobile system with S antennas equipped at the base station side and U antennas configured at the UE side, the data transmission can be expressed as

$$\boldsymbol{y}(t) = \boldsymbol{H}(t)\cdot\boldsymbol{x}(t) + \boldsymbol{n}(t), \tag{2}$$

where $\boldsymbol{x}(t)$ contains the S transmitted signals at base station transceivers; $\boldsymbol{y}(t)$ contains the U received signals at UE receiver inputs; $\boldsymbol{n}(t)$ is the noise vector; $\boldsymbol{H}(t)$ is the channel correlation matrix of U rows and S columns.

The (u,s) component ($u = 1,2,\cdots,U$; $s = 1,2,\cdots,S$) of $\boldsymbol{H}(t)$, marked as $h_{(u,s)}(t)$, indicating the signal change from the sth transmitting port to the uth receiver, is defined as[22,23]

$$h_{(u,s)}(t) = \sum_{n=1}^{N} h_{(n,u,s)}(t), \tag{3}$$

where $h_{(n,u,s)}(t)$ is the nth propagation ray; N is the number of rays defined in the channel model. Channel model is defined as the mathematical descriptions of a physical multi-path environments where wireless UE works, including the microwave propagating directions, reflections caused by buildings, delay, Doppler, the angle arrival, etc. The 3GPP proposes the spatial channel model extension (SCME) for specifying the MIMO mobile phone throughput evaluations.

For generality, a typical 3D channel model proposed in Ref. [23] is adopted here for throughput modeling, where $h_{(n,u,s)}(t)$ is rewritten as

$$h_{(n,u,s)}(t) = \sum_{m=1}^{M} \left(\mathrm{e}^{(-\mathrm{j}2\pi\lambda^{-1} D_s^{tx}(\Omega_{\mathrm{m}}^{tx}))} * \mathrm{e}^{(-\mathrm{j}p\nu t)} * \mathrm{e}^{(-\mathrm{j}2\pi\lambda^{-1} D_u^{rx}(\Omega_n^{rx}))} * \begin{bmatrix} F_u^{rx(V)}(\Omega_n^{rx}) \\ F_u^{rx(H)}(\Omega_n^{rx}) \end{bmatrix}^{\mathrm{T}} \right.$$

Authorized licensed use limited to: HUNAN UNIVERSITY. Downloaded on March 04,2021 at 08:40:01 UTC from IEEE Xplore. Restrictions apply.

$$\left.\begin{bmatrix} \chi_{n,m}^{V,V} & \chi_{n,m}^{V,H} \\ \chi_{n,m}^{H,V} & \chi_{n,m}^{H,H} \end{bmatrix} \cdot \begin{bmatrix} F_s^{tx(V)}(\Omega_{\mathrm{m}}^{tx}) \\ F_s^{tx(H)}(\Omega_{\mathrm{m}}^{tx}) \end{bmatrix} \right), \tag{4}$$

where $F_u^{rx(p)}$ is the uth UE antenna gain in p polarization; $F_u^{tx(p)}$ is the sth base station antenna gain; $\begin{bmatrix} \chi_{n,m}^{V,V} & \chi_{n,m}^{V,H} \\ \chi_{n,m}^{H,V} & \chi_{n,m}^{H,H} \end{bmatrix}$ are the channel complex gains; Ω_{m}^{tx} and Ω_n^{rx} are the angle of arrival and department respectively; $D_s^{tx}(\Omega_{\mathrm{m}}^{tx})$ and $D_u^{rx}(\Omega_n^{rx})$ are the phases offsets; $p\nu$ indicates the Doppler impact. Since the channel is a known mathematical model and the antenna pattern can be measured, $\boldsymbol{H}(t)$ in (2), (3) and (4) can be calculated. While the signal $\boldsymbol{y}(t)$ is achieved, MIMO receivers will recover the transmitted $\boldsymbol{x}(t)$ and then do demodulations. Errors occurred in the demodulation process will lower the overall throughput rate.

Compared to a single receiver configured wireless system, a practical MIMO system performance is related to additional respects. The first factor is the channel correlation matrix achieved through integrating base station antenna patterns, real channel model, and UE antenna patterns, as discussed before. Then are the noise levels at the two receivers. In the paper, it is assumed that the difference between the actual noise power density at the 1st receiver (marked as $n_1(t)$) and N_0 is ΔN_1 dB, and the difference between the actual noise power density at the 2nd receiver (marked as $n_2(t)$) and N_0 is ΔN_2 dB.

A. Impact of Practical Channel Correlation Matrix

The component $h_{ij}(t)$ in $\boldsymbol{H}(t)$ represents the total complex gain from the jth transmitting port to the ith receiver, as shown in Fig. 3. Define the total received power at each receiver as the sum of power levels of two different streams. So the received SNR levels at both receivers (marked as $\mathrm{Snr}_{\mathrm{rx1}}$ and $\mathrm{Snr}_{\mathrm{rx2}}$ can be expressed as

$$\begin{aligned} \mathrm{Snr}_{\mathrm{rx1}} &= P_r - N_0 + 10 * \lg(E[|h_{1,1}(t)|^2] + E[|h_{1,2}(t)|^2]), \\ \mathrm{Snr}_{\mathrm{rx2}} &= P_r - N_0 + 10 * \lg(E[|h_{2,1}(t)|^2] + E[|h_{2,2}(t)|^2])), \end{aligned} \tag{5}$$

where $E[\,]$ denotes the mathematical expectation. And define the MIMO average SNR value as the average value of the two SNR, as

$$\begin{aligned} \mathrm{Snr}_{\mathrm{av}} = 10 * \lg\left((10^{(\mathrm{Snr}_{\mathrm{rx1}}/10)} + 10^{(\mathrm{Snr}_{\mathrm{rx2}}/10)})/2\right) = \\ P_r - N_0 + G_{\mathrm{m}}, \end{aligned} \tag{6}$$

where

$$\begin{aligned} G_{\mathrm{m}} = 10 * \lg\big((E[|h_{1,1}(t)|^2] + E[|h_{1,2}(t)|^2] + \\ E[|h_{2,1}(t)|^2] + E[|h_{2,2}(t)|^2])/2\big). \end{aligned} \tag{7}$$

Although $\mathrm{Snr}_{\mathrm{av}}$ is the defined received average SNR value at the MIMO receivers, it should not be substituted into (1) for throughput calculations. Since after receiving the multiple stream signals, the system requires to do estimation and inversion of the channel correlation matrix, which will additionally amplify the existed noise.

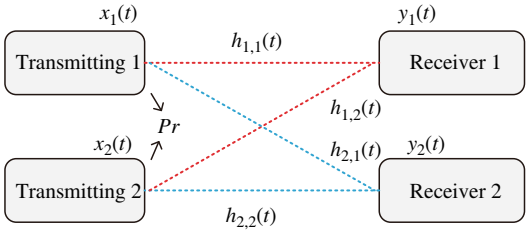

Figure 3 An illustration of the channel correlation matrix in a 2 × 2 MIMO system

The vector transmission in a 2 × 2 MIMO system is rewritten as

$$\begin{aligned} &\boldsymbol{y}(t) = \begin{bmatrix} h_{1,1}(t) & h_{1,2}(t) \\ h_{2,1}(t) & h_{2,2}(t) \end{bmatrix} \cdot \boldsymbol{x}(t) + \boldsymbol{n}(t) = \\ &\begin{bmatrix} 1/f_{\mathrm{m}} & 0 \\ 0 & f_{\mathrm{m}} \end{bmatrix} \cdot \begin{bmatrix} f_{\mathrm{m}} * h_{1,1}(t) & f_{\mathrm{m}} * h_{1,2}(t) \\ 1/f_{\mathrm{m}} * h_{2,1}(t) & 1/f_{\mathrm{m}} * h_{2,2}(t) \end{bmatrix} \cdot \boldsymbol{x}(t) + \boldsymbol{n}(t) = \\ &\boldsymbol{F}_{\mathrm{m}} \cdot \boldsymbol{H}_{fm}(t) \cdot \boldsymbol{x}(t) + \boldsymbol{n}(t), \end{aligned} \tag{8}$$

where

$$\begin{cases} f_{\mathrm{m}} = \sqrt[4]{\dfrac{E[|h_{2,1}(t)|^2] + E[|h_{2,2}(t)|^2]}{E[|h_{1,1}(t)|^2] + E[|h_{1,2}(t)|^2]}}, \\ \boldsymbol{F}_{\mathrm{m}} = \begin{bmatrix} 1/f_{\mathrm{m}} & 0 \\ 0 & f_{\mathrm{m}} \end{bmatrix}, \\ \boldsymbol{H}_{fm}(t) = \begin{bmatrix} f_{\mathrm{m}} * h_{1,1}(t) & f_{\mathrm{m}} * h_{1,2}(t) \\ 1/f_{\mathrm{m}} * h_{2,1}(t) & 1/f_{\mathrm{m}} * h_{2,2}(t) \end{bmatrix}. \end{cases} \tag{9}$$

(8) and (9) give another perspective for describing the 2 × 2 MIMO system, as shown in Fig. 4, where the vector $\boldsymbol{x}(t)$ is processed by $\boldsymbol{H}_{fm}(t)$, $\boldsymbol{F}_{\mathrm{m}}$ and then delivered into the receivers. The received $\mathrm{Snr}_{\mathrm{av}}$ values (defined in (6)) at the marked "B ports" and the receiver inputs are the same, since the defined factor G_{m} is independent on matrix $\boldsymbol{F}_{\mathrm{m}}$. However, inversing the matrix $\boldsymbol{F}_{\mathrm{m}}$ and recovering the vector $\boldsymbol{x}(t)$ (demodulating process) will amplify the existed noise. Theoretically, the larger the norm of the matrix $\boldsymbol{F}_{\mathrm{m}}$ is, the bigger the matrix condition number is, and the larger the degrading impact on the final SNR is. Especially, in case of a norm being one (the minimum limit), $\boldsymbol{F}_{\mathrm{m}}$ will have no influence on the SNR value. By contrast, a norm of positive infinity will result in that the SNR drops drastically and the receiver cannot demodulate. In the proposed model, the SNR value with the impact of factor $\boldsymbol{F}_{\mathrm{m}}$ in consideration is built as

$$\mathrm{Snr}_{\mathrm{av},\boldsymbol{F}_{\mathrm{m}}} \approx \mathrm{Snr}_{\mathrm{av}} - \lg(\mathrm{norm}(\boldsymbol{F}_{\mathrm{m}}, 2)), \tag{10}$$

Authorized licensed use limited to: HUNAN UNIVERSITY. Downloaded on March 04,2021 at 08:40:01 UTC from IEEE Xplore. Restrictions apply.

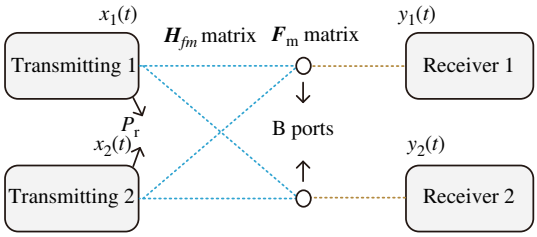

Figure 4 Another equivalent representation of Fig. 3

where norm$(,2)$ is the second order norm of a matrix. While the value of norm$(\boldsymbol{F}_{\mathrm{m}},2)$ reaches its upper and lower limits, the two sides of (10) are strictly equivalent.

Besides the impact caused by $\boldsymbol{F}_{\mathrm{m}}$, the correlation coefficient of $\boldsymbol{H}_{fm}(t)$ should also be considered for its degradation on the received SNR. Referring to (8) in Ref. [23], the correlation coefficient between $h_{k,l}(t)$ and $h_{f,g}(t)$ is defined as

$$\rho_{kl,fg} = \frac{E[h_{k,l}(t)h^*_{f,g}(t)]}{\sqrt{E[|h_{k,l}(t)|^2]*E[|h_{f,g}(t)|^2]}}, \tag{11}$$

where $h_{k,l}(t)$ and $h_{f,g}(t)$ are the (k,l) and (f,g) components in $\boldsymbol{H}(t)$. Since f_{m} in $\boldsymbol{H}_{fm}(t)$ is time-invariant, the correlation coefficient $\rho_{kl,fg}$ in $\boldsymbol{H}_{fm}(t)$ is equivalent to the corresponding value in $\boldsymbol{H}(t)$.

In the paper, we define the transmitting correlation coefficient ρ^{tx} and the receiving correlation coefficient ρ^{rx} as

$$\begin{aligned}
\rho^{tx}_1 &= \frac{E[h_{1,1}(t)h^*_{1,2}(t)]}{\sqrt{E[|h_{1,1}(t)|^2]*E[|h_{1,2}(t)|^2]}},\\
\rho^{tx}_2 &= \frac{E[h_{2,1}(t)h^*_{2,2}(t)]}{\sqrt{E[|h_{2,1}(t)|^2]*E[|h_{2,2}(t)|^2]}},\\
\rho^{rx}_1 &= \frac{E[h_{1,1}(t)h^*_{2,1}(t)]}{\sqrt{E[|h_{1,1}(t)|^2]*E[|h_{2,1}(t)|^2]}},\\
\rho^{rx}_2 &= \frac{E[h_{1,2}(t)h^*_{2,2}(t)]}{\sqrt{E[|h_{1,2}(t)|^2]*E[|h_{2,2}(t)|^2]}},\\
\rho^{tx} &= \sqrt{|\rho^{tx}_1|*|\rho^{tx}_2|},\\
\rho^{rx} &= \sqrt{|\rho^{rx}_1|*|\rho^{rx}_2|},
\end{aligned} \tag{12}$$

where $()^*$ means conjugate transpose.

The correlation coefficient is a finite value that belongs to [0,1]. The smaller the coefficient is, the smaller the caused degradation on throughput performance is. Similar to how the norm of matrix $\boldsymbol{F}_{\mathrm{m}}$ affects the SNR value, a coefficient of zero will have no influence, and a coefficient of one will result in that the receiver cannot demodulate. In the analytical model, the SNR with the impacts of factors $\boldsymbol{F}_{\mathrm{m}}$, ρ^{tx}, and ρ^{rx} in consideration is built as

$$\mathrm{Snr}_{\mathrm{av},\boldsymbol{F}_{\mathrm{m}},\rho} \approx \mathrm{Snr}_{\mathrm{av},\boldsymbol{F}_{\mathrm{m}}} + \lg\left[(1-\rho^{tx})^{\mathrm{K}_2}(1-\rho^{rx})^{\mathrm{K}_3}\right] \tag{13}$$

where K_2 and K_3 are constant.

Finally, in case of $\Delta N_1 = \Delta N_2 = 0$, the MIMO throughput model can be expressed as

$$T_{\mathrm{pm}} \approx R_{\mathrm{m}} * \kappa(\mathrm{Snr}_{\mathrm{av},\boldsymbol{F}_{\mathrm{m}},\rho}). \tag{14}$$

B. Impact of Receiver Noise

For more general cases of $\Delta N_1 \neq 0$ and $\Delta N_2 \neq 0$, assume that the noise power density at the 1st receiver is larger than N_0 by ΔN_1 dB, which means the received SNR of the 1st receiver is degraded by ΔN_1 dB. This situation can also be considered as the received signal power level reduced by ΔN_1 dB with noise level unchanged. The received signal at the 1st receiver is $h_{1,1}(t)*x_1(t)+h_{1,2}(t)*x_2(t)$. Thus, the 1st received power is reduced by ΔN_1 dB, which can be considered as the factors $h_{1,1}(t)$ and $h_{1,2}(t)$ degraded by $\sqrt{10^{(\Delta N_1/10)}}$ times in real. Similarly, the factors $h_{2,1}(t)$ and $h_{2,2}(t)$ are reduced by $\sqrt{10^{(\Delta N_2/10)}}$ times in real. Therefore, in the condition of $\Delta N_1 \neq 0$ and $\Delta N_2 \neq 0$, we can rewrite the factors G_{m} and f_{m} as G^p_{m} and f^p_{m}, separately

$$\begin{aligned}
G^p_{\mathrm{m}} = 10*\lg\Bigg(&\frac{E[|h_{1,1}(t)|^2]+E[|h_{1,2}(t)|^2]}{2*10^{(\Delta N_1/10)}} + \\
&\frac{E[|h_{2,1}(t)|^2]+E[|h_{2,2}(t)|^2]}{2*10^{(\Delta N_2/10)}}\Bigg),
\end{aligned} \tag{15}$$

and

$$f^p_{\mathrm{m}} = \sqrt[4]{\left(\frac{E[|h_{2,1}(t)|^2]+E[|h_{2,2}(t)|^2]}{E[|h_{1,1}(t)|^2]+E[|h_{1,2}(t)|^2]}\right)\frac{10^{(\Delta N_1/10)}}{10^{(\Delta N_2/10)}}}. \tag{16}$$

According to the definitions, ρ^{rx} and ρ^{tx} are independent of ΔN_1 and ΔN_2. Finally, in consideration of cases that $\Delta N_1 \neq 0$, $\Delta N_2 \neq 0$, and $\boldsymbol{H}(t)$ is calculated with antenna patterns and channel model, from (1) (6) (10) (12) (13) (14) (15) and (16), the ultimate throughput model can be expressed as

$$T_{\mathrm{pm}} \approx R_{\mathrm{m}} * \kappa(P_r - N_0 + \Psi), \tag{17}$$

where P_r is the downlink power from the base station,

$$\begin{aligned}
F^p_{\mathrm{m}} &= \begin{bmatrix} 1/f^p_{\mathrm{m}} & 0 \\ 0 & f^p_{\mathrm{m}} \end{bmatrix},\\
\Psi &= G^p_{\mathrm{m}} - 10\lg(\mathrm{norm}(F^p_{\mathrm{m}},2)) + \\
&\quad 10\lg((1-\rho^{tx})^{\mathrm{K}_2}(1-\rho^{rx})^{\mathrm{K}_3}).
\end{aligned}$$

C. Baseline Measurement

As discussed earlier, the function κ is obtained via a process of measurement. A simplified diagram of real-time throughput simulating and testing system is shown in Fig. 5, where the protocol parameters are configured in the base station emulator (BSE) and the UE, the channel information is generated by the channel emulator, including all information about the dynamic channel correlation matrix of $\boldsymbol{H}(t)$. Such

Authorized licensed use limited to: HUNAN UNIVERSITY. Downloaded on March 04,2021 at 08:40:01 UTC from IEEE Xplore. Restrictions apply.

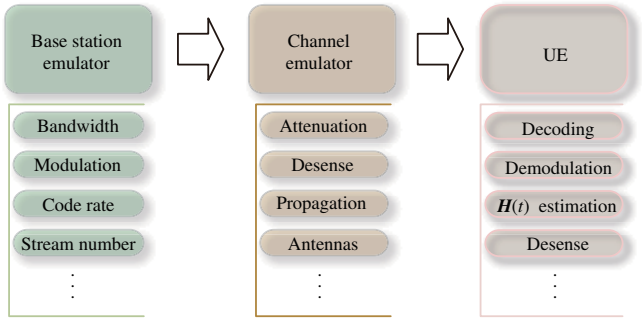

Figure 5 A simplified diagram of real-time throughput simulation and testing system

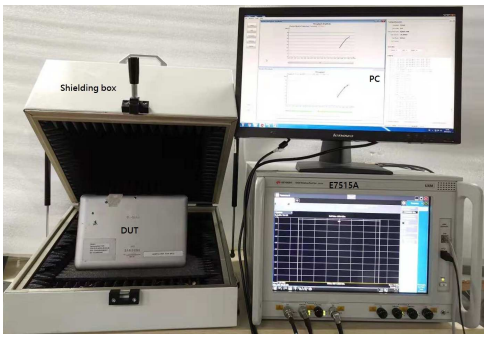

Figure 6 The practical MIMO throughput testing system for the validations in the paper

a system can completely simulate the real use scenarios of the wireless UE. Based on the testing system, the κ is measured via two steps. First, configure the protocol parameters in BSE and UE, and select channel information in channel emulator. Then, set $\boldsymbol{H}(t)$ to be a dynamic low-correlated matrix, and conduct throughput testing via adjusting the transmitted power P_r step by step and obtaining the throughput value in statistics. Achieving the throughput curve at a low-correlated matrix could reduce as much as possible the testing uncertainties caused by channel estimations. It is noted that the noise level at the receiver can be obtained via techniques in Ref. [24]. So the baseline of κ can be clearly depicted.

IV. Validations

A. Modeling

For the model's accuracy validations, a practical throughput model is built in this part based on a testing system shown in Fig. 6, where the BSE and channel emulator are integrated in one instrument E7515A, and a cellular mobile terminal is utilized as the device under test (DUT). The terminal is located in a shielding box and connected to the instrument. Especially, the SCME urban micro (Umi) channel model is selected for validations, which is one of the only two standard models specified by 3GPP and CTIA for 4G long-term evolution (LTE) MIMO over the air (OTA) tests, and will be expanded for further 5G MIMO throughput evaluations. Several major parameters are listed in Tab. 1.

Table 1 Measurement parameters

Parameter	Value
Instruments	PC, Keysight E7515A
DUT	Samsung Tab2
Test protocol	LTE frequency division duplexing (FDD)
Test mode	2 × 2 MIMO (2 streams)
Test channel	SCME Umi
K_2, K_3	0.25, 0.5
Protocol rate	35.424 Mbit/s

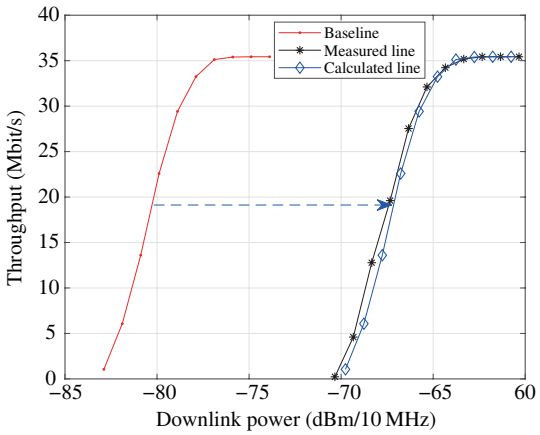

Figure 7 The measured baseline is illustrated in this figure as the red line on the left

Under the configurations, the baseline is measured as illustrated by the red real line in Fig. 7, where the x-axis represents the downlink power, and the y-axis denotes the throughput value. The decomposition parameters for the baseline are given in detail in Tab. 2. It is noted that during the baseline measurement, two omnidirectional, un-correlated, and polarized diversity antennas are used for generating a low correlated channel matrix. And the corresponding factor Ψ in the baseline testing (marked as Ψ_{bs} in the Tab. 2) is provided.

B. Validations

For verifying the accuracy of this model, the case with practical antennas and desense is adopted into the model for comparison between the calculated throughput-power curve and the measured line. The comparison is conducted by following three steps.

1. According to the practical antenna patterns, compute the channel correlation matrix $\boldsymbol{H}(t)$.

2. Achieve the transmitting and receiving correlations ρ^{tx} and ρ^{rx} defined in (12) with the computed matrix $\boldsymbol{H}(t)$.

3. With substituting the acquired $\boldsymbol{H}(t)$ and the noise levels at two receivers into (15) and (16), calculate the values factors G_{m}^{p} and f_{m}^{p}.

Authorized licensed use limited to: HUNAN UNIVERSITY. Downloaded on March 04,2021 at 08:40:01 UTC from IEEE Xplore. Restrictions apply.

Table 2 Measurement parameters for baseline

Parameter	Value
DUT antenna patterns	The 1st antenna is configured to be isotropic and single V-polarized, and the 2nd antenna is configured to be isotropic and only H-polarized
The value of G_{m}^{p}	−0.14 dB (with the channel power normalized)
The value of $10\lg(\mathrm{norm}(\boldsymbol{F}_{\mathrm{m}}^{p},2))$	0.35 dB
The correlation ρ^{tx}	0.112 7
The correlation ρ^{rx}	0.099 7
The noise level at the 1st receiver	−96.6 dBm/10 MHz
The noise level at the 2nd receiver	−95.2 dBm/10 MHz
The value of Ψ_{bs}	−0.99 dB

4. Substitute obtained parameters ρ^{tx}, ρ^{rx}, G_{m}^{p}, f_{m}^{p} into (17) for factor Ψ calculating.

5. Shift the baseline along the x-axis by an offset of $\Psi-\Psi_{\mathrm{bs}}$ to get the throughput function with the actual antenna patterns applied. As shown in Fig. 7, the blue curve shifted from the baseline is the calculated result.

6. Measure the real throughput curve by using the testing system in Fig. 6. Then compare the difference between the measured line and the computed result.

The estimated line is highly consistent with the measured result in Fig. 7. Actually, hundreds of experiments based on different kinds of RF combinations are conducted in the paper. All the factors G_{m}^{p}, F_{m}^{p}, ρ^{tx}, ρ^{rx}, ΔN_1, ΔN_2 are calculated according to the actual RF combinations, as listed in Fig. 8, where the x-axis is the index of RF combination, and the y-axis represents the value of each factor. The differences are analyzed. Especially, for each comparison among calculation and measurement, the power offsets on x-axis that respectively correspond to the three fixed throughput points of $70\%R_{\mathrm{m}}$, $50\%R_{\mathrm{m}}$, $30\%R_{\mathrm{m}}$, are calculated, and marked as $\Delta P_{0.7}$, $\Delta P_{0.5}$, $\Delta P_{0.3}$, which are finally illustrated in Fig. 9.

C. Analysis

The experimental results could hold several conclusions.

1. All the differences are within ±1.25 dB, and 95% of which are within ±0.7 dB. The throughput analytical model has a good correspondence with the actual testing system. Two main uncertainty contributors may impact the comparisons. The first one is the MIMO throughput testing uncertainties, which is discussed in Ref. [14]. In this paper, the provided system has a test repeatability of ±0.3 dB. The second one is the calculation errors on the factors G_{m}^{p}, I_{m}^{p}, ρ^{tx}, ρ^{rx}, which are all computed in a statistical approach. And the throughput value is high-sensitive to the factors ρ^{tx}, ρ^{rx} while the two parameters are close to the upper limitation.

2. According to (1), once the analytical model is built, the

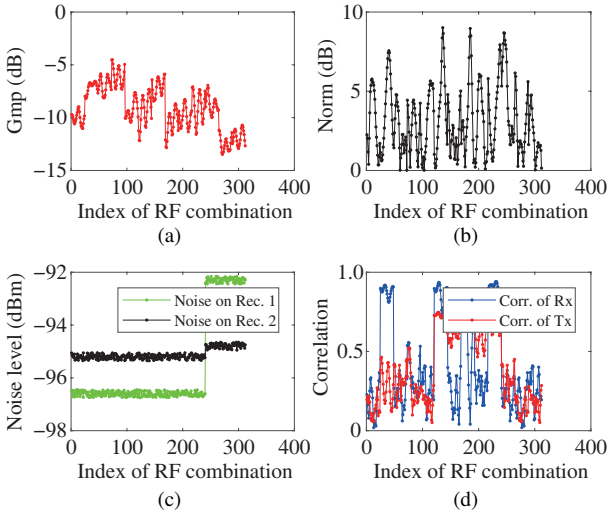

Figure 8 The decomposition parameters shown in this figure are to illustrate that in the experimental verifications, the changes of each parameter are in considerations: (a) average gain; (b) norm of the matrix; (c) noise levels; (d) correlations

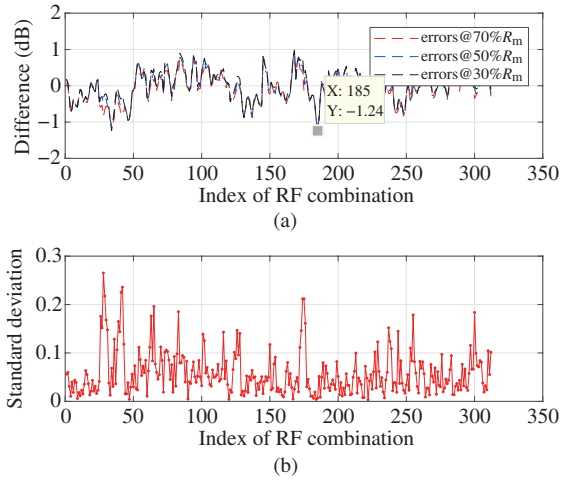

Figure 9 The errors between calculations and measurements and the related standard deviations are listed: (a) differences between calculations and measurements; (b) standard deviation of the differences

throughput curve as a function of power under different RF performances is invariant in shape and has shifted versions in x-axis. Thus theoretically, $\Delta P_{0.7}$, $\Delta P_{0.5}$, $\Delta P_{0.3}$ are equivalent in one comparison. In the paper, the standard deviations of the three errors are provided, as shown in Fig. 9. All the standard deviations are smaller than 0.3 and 95% of them are within 0.15, which is consistent with the theoretical derivations.

V. Application Scenario

Based on the proposed analytical model, the throughput impact caused by each parameter is presented, which is helpful to guide designers to avoid possible risks during wireless system design. Furthermore, combined with the test results in previous sections, a throughput diagnosis report is provided as

Authorized licensed use limited to: HUNAN UNIVERSITY. Downloaded on March 04,2021 at 08:40:01 UTC from IEEE Xplore. Restrictions apply.

Table 3 Measurement results for receiver throughput

Parameter	Value
Related noise level at the 1st receiver	−101.9 dBm/10 MHz
Related noise level at the 2nd receiver	−101.4 dBm/10 MHz
Downlink power corresponding to 70% of the maximum rate	−82.89 dBm/10 MHz (−110.69 dBm/15 KHz)

an example, illustrating how to troubleshoot in a much more effective way.

A. Throughput Impact Related to Receivers

The first concern is the receiver performance. In order to isolate antenna and desense related impact, the receiver is analyzed in the assumptions that two omnidirectional, single-polarized, polarization-diversified antennas are configured, and the external noise could not be coupled and delivered into the receiver inputs. In this case, the acquired throughput performance represents the limit achievable for a system with this receiver configured.

Following the model built in section V, the receiver throughput can be calculated while the noise at receiver inputs is obtained (with desense isolated). Actually, the conducted sensitivity of a receiver can be measured with RF cable connected to receiver directly, and the noise level of each receiver could be further achieved by the procedures described in Ref. [24]. Moreover, in a conductive testing, external noise cannot be coupled into the receiver via antennas, that is, the desense portion is isolated. Substituting the noise and the ideal patterns into the analytical model yields the chip's own throughput performance. For the convenience of comparison, the downlink power corresponding to 70% of the maximum rate is selected as the figure of metric of throughput performance. Then, the receiver performance is listed in Tab. 3, which points out that the value of −110.69 dBm/15 KHz is the upper performance limited by the receivers.

In fact, if the receiver performance could not meet the networking requirement, it means that even if the antenna is ideally un-correlated and there is no self-interference, the performance is still required to be improved. In practice, self-interference and antenna correlation will always degrade the throughput performance. Thus generally, the chip performance should be much better than the requirement of networking.

B. Throughput Impact Related to Antennas

A conventional antenna design will go through an iterative process of "designing-manufacturing-throughput impact testing-improving", which is extremely time-consuming but cannot be neglected, since the relationship between throughput and the conventional antenna specifications (such as envelope correlation coefficient and voltage standing wave ratio) is unknown. That is a common problem of antenna design

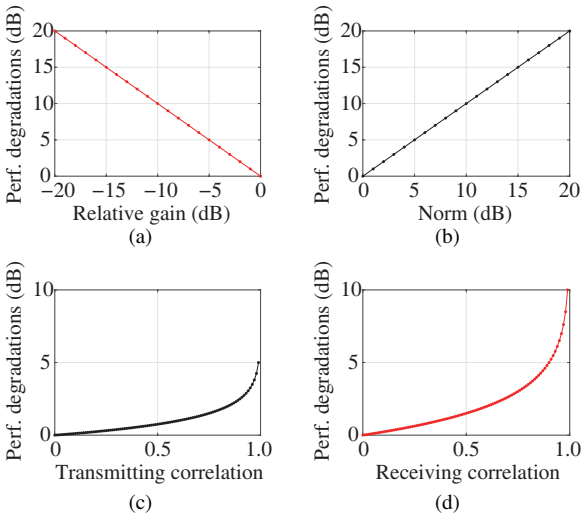

Figure 10 The throughput performance degradations caused by the four antenna-related factors: (a) relationship between throughput sensitivity and the relative gain; (b) the norm; (c) the transmitting correlation; (d) the receiving correlation

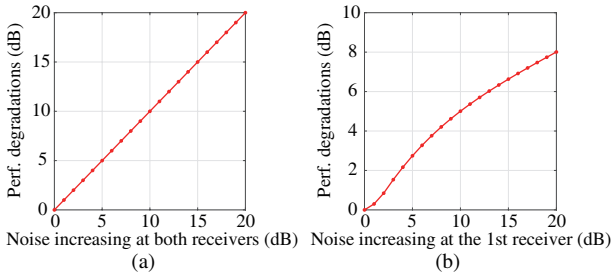

Figure 11 The throughput performance degradation caused by the desense: (a) relationship between throughput sensitivity and the noise levels at both receivers; (b) relationship between throughput sensitivity and the noise level at the 1st receiver

in MIMO systems. Based on the analytical model, the paper defines four indicators for evaluating antennas: relative gain (defined in (15) and related to the value in baseline), norm (defined in (9)), transmitting correlation (defined in (12)), and receiving correlation (defined in (12)). And their contributions to the throughput are provided. Following the previous model example, throughput performance degradations caused by the four factors are given, as shown in Fig. 10.

From the figure, increasing the relative gain or reducing the norm can linearly improve the throughput performance. In case of a high correlation level, the throughput rate will drop sharply with the correlation increased, especially with the receiving correlation raising. It is the first time that engineers can directly estimate the degradation of throughput performance with the MIMO antennas applied during the R&D stage, which will significantly reduce the number of iterations of antenna design.

C. Throughput Impact Related to Desense

The interference inside DUT would be coupled via antennas and then delivered into receivers, which is how the desense

Authorized licensed use limited to: HUNAN UNIVERSITY. Downloaded on March 04,2021 at 08:40:01 UTC from IEEE Xplore. Restrictions apply.

Table 4 Throughput diagnosis report of the 240th validation result

Sub-system	Decomposition parameter and its impact			Throughput performance
	Factors	Value	Degradation	
Receiver	Noise on the 1st receiver	−101.90 dBm/10 MHz	–	−110.69 dBm/15 KHz
	Noise on the 2nd receiver	−101.40 dBm/10 MHz	–	
Antennas	Relative gain	−7.71 dB	7.71 dB	−96.11 dBm/15 KHz
	Norm	1.35 dB	1.35 dB	
	Transmitting correlation	0.68	1.24 dB	
	Receiving correlation	0.86	4.27 dB	

emerges. Increasing noise level at each receiver is equivalent to reducing the corresponding antenna gain, as stated before. With the loaded antenna patterns fixed, we can achieve the throughput performance degradation along to the changing noise. As shown in Fig. 11, the left figure illustrates the degradation caused by a synchronous noise increasing at both receivers, and the right figure illustrates the degradation caused by a single noise increasing at the 1st receiver.

D. Throughput Diagnosis Report

Take the 240th validating result in section V as an example to analyze its diagnosis report. The diagnosis measurement is conducted in following steps.

1. Obtain the noise levels at both the receivers and then measure the throughput result, in a conductive approach, as shown in Tab. 4, where −110.69 dBm/15 KHz is the upper limitation with the receivers configured.

2. Measure the DUT antenna patterns, and calculate the parameters: G_{m}^{p}, F_{m}^{p}, ρ^{tx}, ρ^{rx}. And finally, compute the degradation caused by the antenna factors. Actually, with the practical antennas equipped, a degradation of 14.57 dB is reached.

3. Achieve the noise level at both the receivers while the DUT is in the integrated configuration, and compute the degradation caused by the desense factors. Finally, with the desense in consideration, the total degradation is 17.9 dB, and the entire throughput performance is −92.79 dBm/15 KHz.

VI. Conclusion

Throughput reflects a communication system's true user experience, which is defined in a perspective of measurement in the 3GPP standardizations. In the paper, it is the first time that throughput is analyzed via a mathematical model with the RF hardware performance included. The model considers both transmission specifications about bandwidth, coding rate, modulation, cyclic prefix, and the radio frequency parameters on antenna correlation, desense, propagation, etc. that output the practical throughput reflecting the achievable data rate of a MIMO system in its realistic application stage. The outputted detailed diagnostic report of a communication system can directly guide designers to avoid disadvantages during wireless system design and optimization for the RF front end improvements. Especially for 5G and Internet of things, where MIMO is the basic technique for holding a high rate and stable network, the mathematic analytical method will make MIMO performance much more predictable during the design phase.

References

[1] SUN S, RAPPAPORT T, SHAFI M, et al. Propagation models and performance evaluation for 5G millimeter-wave bands[J]. IEEE Trans. Veh. Technol., 2018, 67(9): 8422-8439.

[2] MESLEH R, HAAS H, SINANOVIC S, et al. Spatial modulation [J]. IEEE Trans. Veh. Technol., 2008, 57(4): 2228-2241.

[3] ZHANG H, JIANG C, BEAULIEU N, et al. Resource allocation for cognitive small cell networks: A cooperative bargaining game theoretic approach[J]. IEEE Trans. Wireless Commun., 2015, 14(6): 3481-3493.

[4] DING Z G, FAN P Z, POOR V. Impact of user pairing on 5G nonorthogonal multiple-access downlink transmissions[J]. IEEE Trans. Wireless Commun., 2016, 65(8): 6010-6023.

[5] YU T Q, WANG X B, SHAMI A. UAV-enabled spatial data sampling in large-scale IoT systems using denoising autoencoder veural network[J]. IEEE Internet Things J., 2019, 6(2): 1856-1865.

[6] LIU X, LIU Y N, WANG X B, et al. Highly efficient 3-D resource allocation techniques in 5G for NOMA-enabled massive MIMO and relaying systems[J]. IEEE J. Sel. Areas Commun., 2014, 35(12): 2785-2797.

[7] QI Y H, YANG G, LIU L, et al. 5G over-the-air measurement challenges: overview[J]. IEEE Trans. Electromagn. Compat., 2017, 59(6): 1661-1670.

[8] 3GPP. Verification of radiated multi-antenna reception performance of User Equipment (UE)[S]. Tech. Report TR 37.977, Revision 15.0.0, 2018: 9.

[9] CHEN J S, STERN T E. Throughput analysis, optimal buffer allocation, and traffic imbalance study of a generic nonblocking packet switch[J]. IEEE J. Sel. Areas Commun., 1991, 9(3): 439-449.

[10] PRASAD R. CDMA for wireless personal communications[M]. Boston: Artech House Publishers, 1996.

[11] PUPALA R N, GREENSTEIN L J, DAUT D G. Effects of channel dispersion and path correlations on system-wide throughput in MIMO-based cellular systems[J]. IEEE Trans. Wireless Commun., 2009, 8(11): 5477-5482.

[12] RHEE C, KIM Y J, PARK T, et al. Pattern-reconfigurable MIMO antenna for high isolation and low correlation[J]. IEEE Antennas Wireless Propag. Lett., 2014, 13: 1373-1376.

[13] 3GPP. User equipment (UE) over the air (OTA) performance; conformance testing[S]. Tech. Specif. TS 37.544 v14.5.0, 2018.

Authorized licensed use limited to: HUNAN UNIVERSITY. Downloaded on March 04,2021 at 08:40:01 UTC from IEEE Xplore. Restrictions apply.

[14] CTIA, Washington, DC, USA. Test plan for 2 × 2 downlink MIMO and transmit diversity over-the-air performanc[S]. Revision 1.1, Aug. 2016.
[15] SHEN P H, QI Y H, YU W, et al. OTA measurement for IoT wireless device performance evaluation: Challenges and solutions[J]. IEEE Internet Things J., 2019, 6(1): 1223-1237.
[16] QI Y H, YU W. Unified antenna temperature[J]. IEEE Trans. Electromagn. Compat., 2016, 58(5).
[17] YU W, QI Y H, LIU K F, et al. Radiated two-stage method for LTE MIMO user[J]. IEEE Trans. Electromagn. Compat., 2014, 56(6): 1691-1696.
[18] SHI L, ZHANG W, XIA X G. On designs of full diversity space-time block codes for two-user MIMO interference channels[J]. IEEE Trans. Wireless Commun., 2012, 11(11): 4184-4191.
[19] MENG Y, ZHANG W, ZHU H J, et al. Securing consumer IoT in the smart home: Architecture, challenges, and countermeasures[J]. IEEE Wireless Commun., 2018, 25(6): 53-59.
[20] PROAKIS J. Digital communications[M]. New York: McGraw-Hill, 1983.
[21] NGO H Q. Massive MIMO: Fundamentals and System Designs[M]. Linköping: LiU-Tryck, 2015.
[22] SHEN P H, QI Y H, YU W, et al. An RTS-based near-field MIMO measurement solutionła step toward 5G[J]. IEEE Trans. Microw. Theory Techn., 2019, 67(7): 2884-2893.
[23] DAO M T, NGUYEN V A, IM Y T, et al. 3D polarized channel modeling and performance comparison of MIMO antenna configurations with different polarizations[J]. IEEE Trans. Antennas Propag., 2011, 59(7): 2672-2682.
[24] SHEN P H, QI Y H, YU W, et al. A decomposition method for MIMO OTA performance evaluation[J]. IEEE Trans. Veh. Technol., 2019, 67(9): 8184-8191.

About the Authors

Penghui Shen received his B.S. and M.S. degrees in electronic information and technology from the Hunan University, Changsha, China, in 2013 and 2016. He is currently working toward his Ph.D. degree in electronics from the same university. His research interests include SISO, MIMO and 5G array measurements for wireless devices, EMC, and antenna design.

Yihong Qi [corresponding author] received his B.S. degree in electronics from National University of Defense Technologies, Changsha, China, in 1982, his M.S. degree in electronics from China Academy of Space Technology, Beijing, China, in 1985, and his Ph.D. degree in Electronics from Xidian University, Xi'an, China, in 1989. From 1989 to 1993, he was a postdoctoral fellow and then an associate professor with Southeast University, Nanjing, China. From 1993 to 1995, he was a postdoctoral researcher at McMaster University, Hamilton, ON, Canada. From 1995 to 2010, he was with Research in Motion (Blackberry), Waterloo, ON, where he was the director of Advanced Electromagnetic Research. Currently, he is the president and a chief scientist with General Test Systems, Inc.; he founded DBJay in 2011. He is also an adjunct professor in EMC Laboratory, Missouri University of Science and Technology, Rolla, MO and an adjunct professor in Hunan University, Changsha, China. He is an honorary professor and the dean of Behivioral Big Data Institute in Southwest University. He is an inventor of more than 400 published and pending patents. Dr. Qi was a distinguished lecturer of IEEE EMC Society for 2014 and 2015, and serves as the chairman of IEEE EMC TC-12. He has received an IEEE EMC Society Technical Achievement Award in August 2017. He is a fellow of Canadian Academy of Engineering.

Xianbin Wang is a professor and Tier 1 Canada Research Chair at Western University, Canada. He received his Ph.D. degree in electrical and computer engineering from National University of Singapore in 2001.

Prior to joining Western, he was with Communications Research Centre Canada (CRC) as a research scientist/senior research scientist between July 2002 and December 2007. From January 2001 to July 2002, he was a system designer at STMicroelectronics. His current research interests include 5G and beyond, Internet-of-things, communications security, machine learning and intelligent communications. Dr. Wang has over 400 peer-reviewed journal and conference papers, in addition to 30 granted and pending patents and several standard contributions.

Dr. Wang is a fellow of Canadian Academy of Engineering, a fellow of Engineering Institute of Canada, a fellow of IEEE and an IEEE distinguished lecturer. He has received many awards and recognitions, including Canada Research Chair, CRC President's Excellence Award, Canadian Federal Government Public Service Award, Ontario Early Researcher Award and 6 IEEE Best Paper Awards. He currently serves as an editor/associate editor for IEEE Transactions on Communications, IEEE Transactions on Broadcasting, and IEEE Transactions on Vehicular Technology. He was also an associate editor for IEEE Transactions on Wireless Communications between 2007 and 2011, and IEEE Wireless Communications Letters between 2011 and 2016. He was involved in many IEEE conferences including GLOBECOM, ICC, VTC, PIMRC, WCNC and CWIT, in different roles such as symposium chair, tutorial instructor, track chair, session chair and TPC co-chair. Dr. Wang is currently serving as the chair of ComSoc Signal Processing for Communications and Computing Technical Committee.

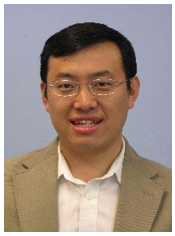

Wei Zhang received his Ph.D. degree in electronic engineering from the Chinese University of Hong Kong, Hong Kong, China in 2005. He was a research fellow with the Hong Kong University of Science and Technology from 2006 to 2007. Currently, he is a professor with the University of New South Wales, Sydney, Australia. His current research interests include 5G, space information networks, and network security. He is an area editor for IEEE Transactions on Wireless Communications and the editor-in-chief of Journal of Communications and Information Networks. He is the vice director of IEEE Communications Society Asia Pacific Board and the chair of IEEE Wireless Communications Technical Committee. He is a member of Board of Governors of IEEE Communications Society and an IEEE fellow.

Wei Yu received his B.S. degree in electrical engineering from Xi'an Jiaotong University, Xi'an, China, in 1991, his M.S. degree in electrical engineering from China Academy of Space Technology (CAST), Beijing, China, in 1994, and his Ph.D. degree in electrical engineering from Xidian University, Xi'an, China, in 2000. From 2001 to 2003, he was a postdoctoral fellow with University of Waterloo, Canada. He was a CTO with Sunway Communications Ltd., from 2008 to 2012. He founded Autonovation Electronics Inc. in 2004 and cofounded General Test Systems Inc., Shenzhen, China, in 2012. He is now with DBJ Technologies as COO. His current research interests include signal processing and mobile device test system. He is an inventor of 91 published and pending patents.

Authorized licensed use limited to: HUNAN UNIVERSITY. Downloaded on March 04,2021 at 08:40:01 UTC from IEEE Xplore. Restrictions apply.